nature structural & molecular biology

APC15 mediates CDC20 autoubiquitylation by APC/C^{MCC} and disassembly of the mitotic checkpoint complex

Kristina Uzunova[1,7], Billy T Dye[2,3,7], Hannelore Schutz[1,7], Rene Ladurner[1], Georg Petzold[1], Yusuke Toyoda[4], Marc A Jarvis[1], Nicholas G Brown[2], Ina Poser[4], Maria Novatchkova[1], Karl Mechtler[1], Anthony A Hyman[4], Holger Stark[5,6], Brenda A Schulman[2,3] & Jan-Michael Peters[1]

The anaphase-promoting complex/cyclosome (APC/C) bound to CDC20 (APC/C^{CDC20}) initiates anaphase by ubiquitylating B-type cyclins and securin. During chromosome bi-orientation, CDC20 assembles with MAD2, BUBR1 and BUB3 into a mitotic checkpoint complex (MCC) that inhibits substrate recruitment to the APC/C. APC/C activation depends on MCC disassembly, which was proposed to require CDC20 autoubiquitylation. Here we characterize APC15, a human APC/C subunit related to yeast Mnd2. APC15 is located near APC/C's MCC binding site; it is required for APC/C-bound MCC (APC/C^{MCC})-dependent CDC20 autoubiquitylation and degradation and for timely anaphase initiation but is dispensable for substrate ubiquitylation by APC/C^{CDC20} and APC/C^{CDH1}. Our results support the model wherein MCC is continuously assembled and disassembled to enable rapid activation of APC/C^{CDC20} and CDC20 autoubiquitylation promotes MCC disassembly. We propose that APC15 and Mnd2 negatively regulate APC/C coactivators and report generation of recombinant human APC/C.

The spindle assembly checkpoint (SAC) delays chromosome segregation until all chromosomes are bi-oriented on the mitotic or meiotic spindle (reviewed in ref. 1). Defects in this surveillance mechanism can lead to chromosome mis-segregation and aneuploidy, a condition associated with congenital trisomies, tumorigenesis and aging. The checkpoint is activated in prometaphase by chromosomes whose kinetochores are not attached or are incorrectly attached to microtubules[2,3]. The checkpoint inhibits CDC20, a protein that associates with and activates the APC/C in mitosis[4–8]. APC/C initiates chromosome segregation by ubiquitylating securin, an inhibitor of the protease separase, and B-type cyclins, activators of cyclin-dependent kinase 1 (CDK1). The subsequent degradation of these proteins by the 26S proteasome leads to activation of separase, which destroys sister-chromatid cohesion and thereby initiates anaphase (reviewed in ref. 9).

The APC/C is a 1.5-MDa protein complex composed of three structural domains, called the 'arc lamp', the 'platform' and the 'catalytic core'[10,11]. The latter domain contains the cullin APC2 and the RING finger subunit APC11 (refs. 10,12). APC11 interacts with ubiquitin-conjugating (E2) enzymes and thereby facilitates the transfer of activated ubiquitin residues from the E2 to APC/C substrates[13–15]. Substrates contain APC/C recognition sequences, called the destruction box (D box)[16] and KEN box[17]. These 'degrons' are thought to be simultaneously recognized by the APC/C subunit APC10 and either CDC20 or CDH1, a CDC20-related coactivator protein that associates with the APC/C in late mitosis and G1 phase[12,18–20].

The SAC inhibits CDC20 by promoting its association with three other proteins, MAD2, BUB3 and BUBR1 (also known as BUB1B and, in fission yeast, as Mad3), which leads to the formation of an MCC[21]. A rate-limiting step in MCC assembly is the binding of CDC20 to MAD2. This process requires conversion of MAD2 from an open (MAD2^{O}) to a closed conformation (MAD2^{C}) in which MAD2^{C} stably embraces CDC20 through a 'safety belt' mechanism[22,23]. The generation of CDC20–MAD2^{C} complexes occurs at checkpoint-active kinetochores to which MAD2^{C} is recruited by binding to MAD1. This MAD1–MAD2^{C} complex promotes conversion of MAD2^{O} to MAD2^{C} and binding of the latter to CDC20. This process is thought to require the transient formation of a conformational MAD2^{O}-MAD2^{C} heterodimer, in which MAD2^{O} is recruited to the MAD2^{C} subunit of the kinetochore-associated MAD1–MAD2^{C} complex[24,25].

MCC can associate with the APC/C, but unlike APC/C^{CDC20}, APC/C^{MCC} is unable to bind and ubiquitylate securin and B-type cyclins[11]. MCC might inhibit CDC20 through multiple mechanisms: a KEN box in Mad3 occupies the KEN box–receptor site on Cdc20 (refs. 20,26), another Mad3 domain might partially block a putative D-box–receptor site on Cdc20 (ref. 20), and CDC20 occupies different positions on the APC/C in the presence or absence of the other MCC subunits[11]. To allow APC/C activation, MCC therefore has to be replaced by CDC20. Several studies have observed that this depends on MCC disassembly (described below). MCC disassembly is an

[1]Research Institute of Molecular Pathology, Vienna, Austria. [2]Department of Structural Biology, St. Jude Children's Research Hospital, Memphis, Tennessee, USA. [3]Howard Hughes Medical Institute, St. Jude Children's Research Hospital, Memphis, Tennessee, USA. [4]Max Planck Institute for Molecular Cell Biology and Genetics, Dresden, Germany. [5]Max Planck Institute for Biophysical Chemistry, Göttingen, Germany. [6]Department of 3D Electron Cryomicroscopy, Institute of Microbiology and Genetics, Georg-August Universität, Göttingen, Germany. [7]These authors contributed equally to this work. Correspondence should be addressed to B.A.S. (brenda.schulman@stjude.org) or J.-M.P. (jan-michael.peters@imp.ac.at).

Received 6 August; accepted 14 September; published online 24 September 2012; doi:10.1038/nsmb.2412

energy-dependent process[27,28], possibly because spontaneous release of CDC20 from MAD2 would be too slow to allow rapid APC/C activation in metaphase[29].

Several mechanisms have been discussed for how MCC may be disassembled. A previous study proposed that CDC20 autoubiquitylation by APC/C^{MCC} leads to MCC disassembly[27]. However, this view has been challenged by another study that observed that CDC20 is continuously synthesized and degraded during prometaphase and proposed that ubiquitin-mediated CDC20 degradation is required to keep CDC20 levels below a threshold that would over-ride the checkpoint[30]. Several studies have shown that MCC disassembly depends on CUEDC2 (ref. 31) and p31(comet)[27,29,32–34] and that CDK1-mediated phosphorylation of these proteins and of CDC20 promotes MCC disassembly[31,35]. CUEDC2's mechanism of action is unknown, but p31(comet) structurally mimics MAD2^{O}, and it can therefore bind to MAD2^{C} (refs. 36,37). This interaction might facilitate dissociation of MAD2^{C} from CDC20.

Here we have characterized the function of C11ORF51, a protein required for mitotic progression[38] and associated with the APC/C[39]. We show that C11ORF51 is a subunit of APC/C's platform domain and is located near the MCC-binding site on the APC/C[11]. As recently reported by another study[40], we find that depletion of C11ORF51, which has been renamed APC15, reduces the rate of MCC disassembly. In addition, we show for the first time, to our knowledge, that APC15 is required for efficient ubiquitylation of CDC20 as part of APC/C^{MCC} and for CDC20 degradation in prometaphase, even though APC15 is not required for substrate ubiquitylation by APC/C^{CDC20} or APC/C^{CDH1}. Our results support the view[27,29] that CDC20 autoubiquitylation contributes to MCC disassembly and that continuous CDC20 synthesis and degradation facilitates rapid APC/C activation in metaphase. In this study, we also report the first generation and characterization, to our knowledge, of recombinant human APC/C, assembled from 14 core subunits and either CDC20 or CDH1.

RESULTS

C11ORF51 (APC15) is a subunit of APC/C's platform domain

As part of the MitoCheck project, we performed a large-scale proteomic study to identify and characterize protein complexes required for mitosis in human cells[41]. This led to the discovery of two previously unknown APC/C interactors, chromosome 10 open reading frame 104 (C10ORF104; ref. 41) and chromosome 11 open reading frame 51 (C11ORF51; ref. 39). C10ORF104 is an 11.7-kDa subunit of APC/C's arc-lamp domain and is now called APC16 (refs. 41,42).

To test whether C11ORF51 is also a subunit of the APC/C, we raised antibodies to this protein. In addition we tagged human *C11ORF51* with a sequence encoding a C-terminal localization affinity-purification (LAP) tag, which contains enhanced green fluorescent protein (EGFP)[43,44], and generated HeLa cells that stably express C11ORF51-LAP. When APC/C was immunoprecipitated from these cells by using CDC27 antibodies, both endogenous and LAP-tagged C11ORF51 could be detected by immunoblotting (**Fig. 1a**), and the bands showed migration rates corresponding to 20 kDa and 55 kDa, respectively. Depletion of endogenous C11ORF51 with four different short interfering RNAs (siRNAs) confirmed that the 20-kDa band recognized by our antibodies corresponds to C11ORF51.

When C11ORF51-LAP was isolated by tandem affinity purification from HeLa cells and analyzed by mass spectrometry, peptides from ten APC/C subunits and CDC20 were identified, which confirmed that C11ORF51 is specifically associated with the APC/C (**Fig. 1b**). In addition, immunoprecipitates obtained with C11ORF51 antibodies contained a similar set of proteins as APC/C samples isolated with CDC27 antibodies, as seen by SDS-PAGE and silver staining (**Fig. 1c**). The C11ORF51

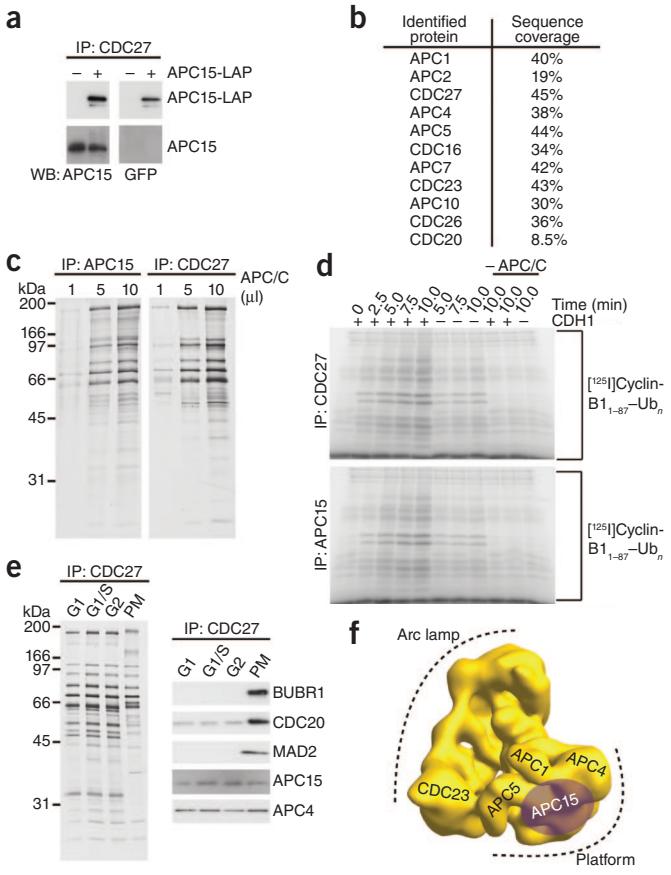

Figure 1 C11ORF51 (APC15) is a subunit of APC/C's platform domain. (**a**) Western blot showing APC/C immunoprecipitations from asynchronous cells or cells expressing APC15-LAP. IP, immunoprecipitation; WB, western blot. (**b**) APC/C subunits identified by mass spectrometry after tandem affinity purification of APC15-LAP. Percentage of peptide sequence coverage of each subunit is listed. (**c**) SDS-PAGE and silver stain showing APC/C immunoprecipitations using APC15 or CDC27 antibodies. (**d**) Autoradiography after *in vitro* ubiquitylation of [I^{125}]-labeled human cyclin-B1 fragment (residues 1–87) by APC/C. APC/C concentration used in this assay was normalized on the basis of APC/C subunit silver-staining intensity shown in **c**. (**e**) SDS-PAGE and silver stain or western blot analysis after APC/C immunoprecipitation from cells arrested in different cell-cycle stages. PM, prometaphase. Ub$_n$ denotes polyubiquitination. (**f**) Three-dimensional model of human APC/C obtained by electron microscopy[11], showing the location of APC15 as determined by antibody labeling.

and CDC27 immunoprecipitates were able to support cyclin-B1 ubiquitylation reactions to similar extents (**Fig. 1d**). Further analysis revealed that C11ORF51 is associated with APC/C in cells synchronized in G1, S, G2 and prometaphase (**Fig. 1e**). These observations indicate that C11ORF51 is a bona fide subunit of the human APC/C.

We next tested whether C11ORF51 is related to subunits of APC/C that have so far only been identified in lower eukaryotes, for example Apc9 or Mnd2 (Apc15) in budding yeast[45,46]. The sequence of C11ORF51 is well conserved among metazoans, ranging from cnidarians to mammals. We used a hidden Markov model (HMM) obtained by multiple sequence alignment of these sequences to search for related proteins in fungal and plant proteomes. We identified sequences significantly related to metazoan C11ORF51 in plants and fungi, with the closest relative of C11ORF51 in *Schizosaccharomyces pombe* being Apc15, an ortholog of *Saccharomyces cerevisiae* Mnd2 (**Supplementary Fig. 1a**,**b**). A reciprocal search in the human, mouse and *Arabidopsis thaliana*

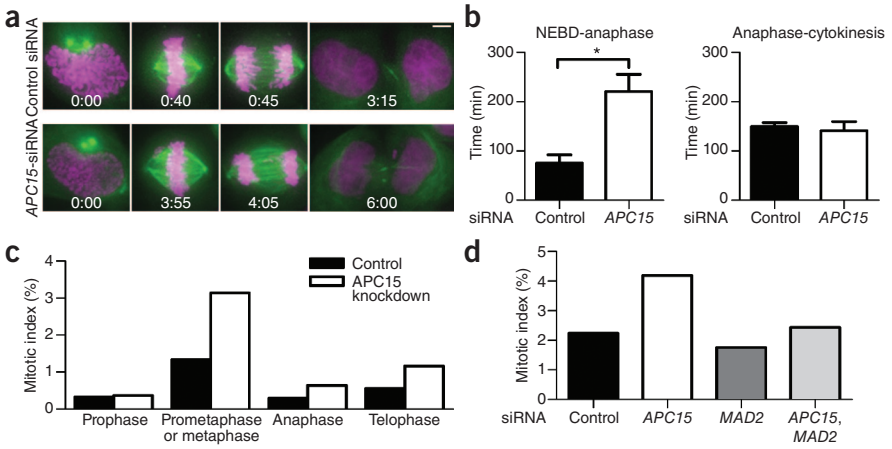

Figure 2 APC15 depletion causes delay in mitosis. (**a**) Still images of time-lapse microscopy experiments showing representative cells at NEBD, metaphase, anaphase and telophase (from left to right). Time of progression for control or *APC15*-siRNA–treated cells after NEBD (h:min) is indicated for the respective cell-cycle stages. Scale bar, 5 μm. Magenta, H2B-mCherry; green, β-tubulin. (**b**) Quantification of the time-lapse microscopy data, showing average times of progression of control or *APC15*-siRNA–treated cells from NEBD to anaphase and from anaphase to cytokinesis ($n = 25$; error bars, s.e.m.; $^*P$ value = 0.0005 from a two-tailed t-test). (**c**) Quantification of mitotic stages after control or *APC15*-siRNA treatment ($n > 8{,}600$ per condition). Staining of CDC20, BUB1, α-tubulin and DNA was used to distinguish between mitotic stages. (**d**) Quantification of mitotic index after treatment with control or *APC15*-siRNA or/and *MAD2*-siRNA ($n = 5{,}000$ per condition). Staining of phosphorylated histone-H3 Ser10, α-tubulin and DNA was used to distinguish between mitotic and interphase cells.

proteomes with an HMM derived from an alignment of *S. pombe* and *Agaricomycetes* Apc15 confirmed that C11ORF51 in metazoans is related to Mnd2 in fungi. It is therefore possible that C11ORF51 and Mnd2 are derived from a common ancestral APC/C subunit. As did a previous study[40], we will refer to C11ORF51 as APC15.

To analyze where APC15 is located within the APC/C, we labeled purified human APC/C with APC15 antibodies under conditions that induce antibody-dependent APC/C dimerization[10–12], isolated the APC/C dimers by density-gradient centrifugation and analyzed them by negative-staining electron microscopy (**Supplementary Fig. 1c**,**d**). The angular orientation of APC/C monomers within the dimers indicates that APC15 is part of APC/C's platform domain, where it might be located in close vicinity to APC4, APC5 and APC1 (**Fig. 1f**). This location is consistent with the possibility that human C11ORF51 is related to yeast Mnd2, given that a previous study[46] used an *in vitro* transcription-translation system and found that Mnd2 interacts with Apc1 and Apc5, which are components of the platform domain, and with Cdc23, which is located close to the platform[11,47].

APC15 is required for anaphase

A previous genome-wide RNA interference (RNAi) screen had shown that depletion of C11ORF51 (APC15) delays mitotic progression[38]. To analyze the function of APC15 further, we depleted this protein by RNAi in HeLa cells stably expressing the histone H2B tagged with mCherry (H2B-mCherry) and β-tubulin tagged with the LAP tag (TUBB-LAP) and performed time-lapse fluorescence microscopy analysis (**Fig. 2a**).

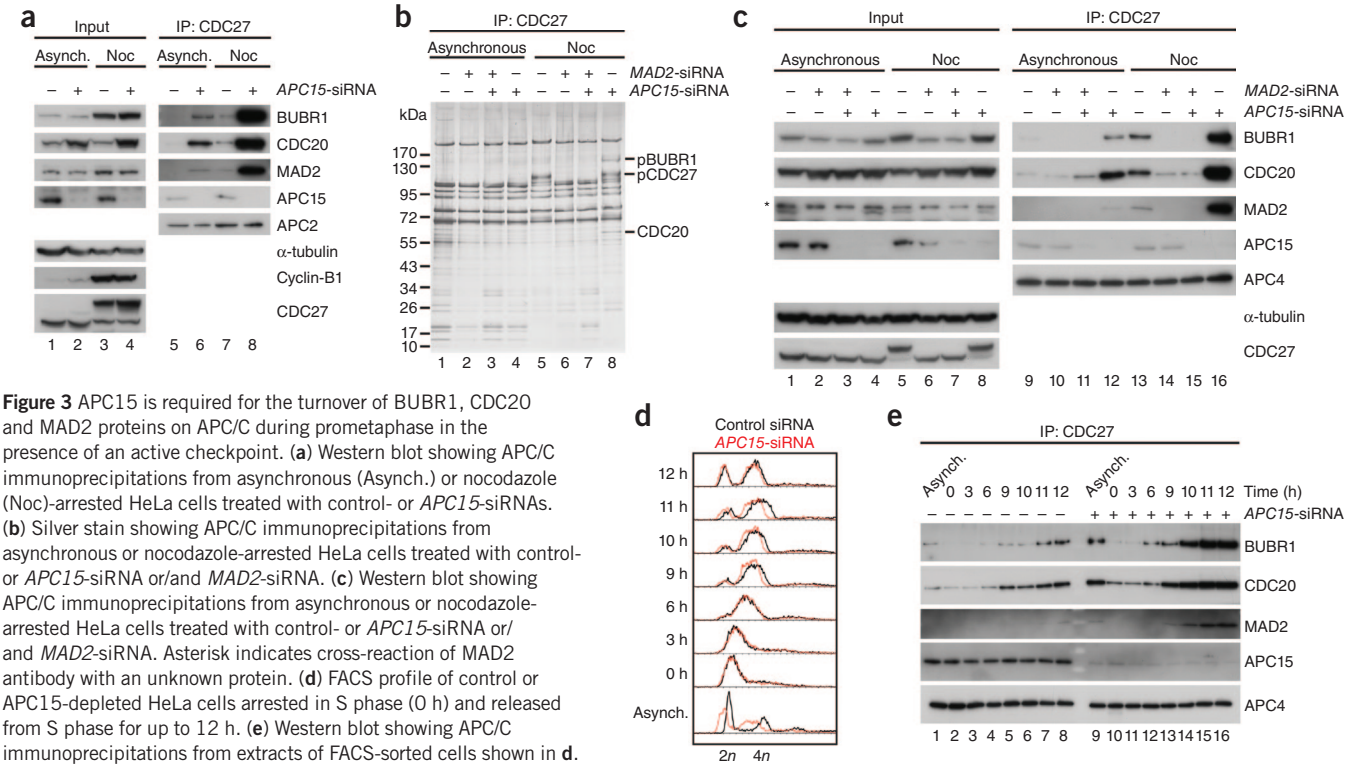

Figure 3 APC15 is required for the turnover of BUBR1, CDC20 and MAD2 proteins on APC/C during prometaphase in the presence of an active checkpoint. (**a**) Western blot showing APC/C immunoprecipitations from asynchronous (Asynch.) or nocodazole (Noc)-arrested HeLa cells treated with control- or *APC15*-siRNAs. (**b**) Silver stain showing APC/C immunoprecipitations from asynchronous or nocodazole-arrested HeLa cells treated with control- or *APC15*-siRNA or/and *MAD2*-siRNA. (**c**) Western blot showing APC/C immunoprecipitations from asynchronous or nocodazole-arrested HeLa cells treated with control- or *APC15*-siRNA or/and *MAD2*-siRNA. Asterisk indicates cross-reaction of MAD2 antibody with an unknown protein. (**d**) FACS profile of control or APC15-depleted HeLa cells arrested in S phase (0 h) and released from S phase for up to 12 h. (**e**) Western blot showing APC/C immunoprecipitations from extracts of FACS-sorted cells shown in **d**.

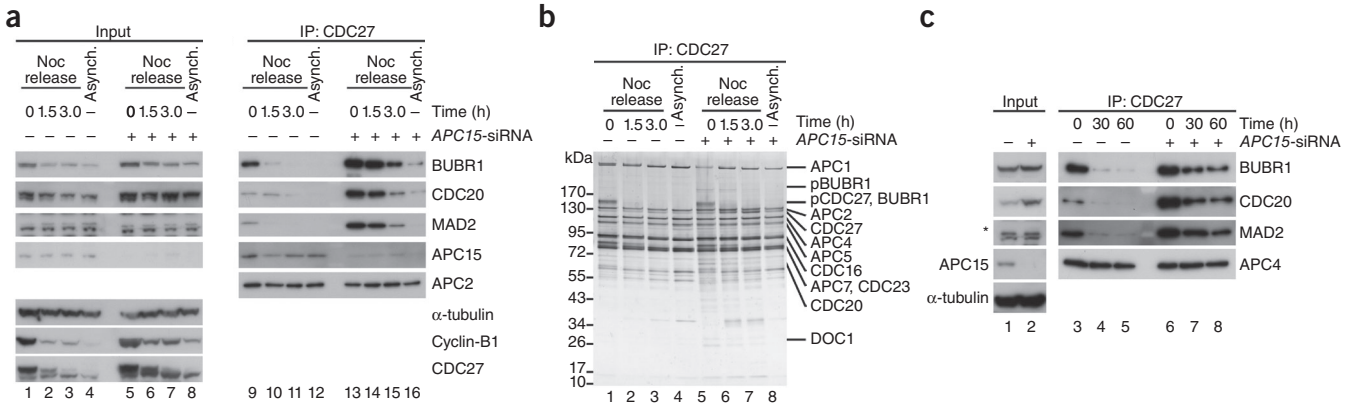

Figure 4 APC15 is required for MCC disassembly *in vivo* and *in vitro*. (**a**) Western blot showing MCC disassembly *in vivo*. Control and APC15-depleted HeLa cells were arrested in prometaphase and released from nocodazole arrest (Noc release) for indicated times. APC/C immunoprecipitates from cells released from nocodazole arrest are shown on the right. (**b**) Silver stain of APC/C immunoprecipitates from cells released from nocodazole arrest. pBUBR1, phosphorylated BUBR1; pCDC27, phosphorylated CDC27. (**c**) Western blot showing *in vitro* MCC disassembly by using APC/C immunoprecipitated from cells arrested in prometaphase. APC/C immobilized on anti-CDC27–antibody beads was incubated with a ubiquitylation mixture for indicated times, washed and eluted by using antigenic peptides. Asterisk indicates cross-reaction of MAD2 antibody with an unknown protein.

In APC15-depleted cells, progression from nuclear-envelope breakdown (NEBD) to anaphase onset took more than twice as long as in control transfected cells, whereas progression from anaphase to cytokinesis was not significantly delayed (**Fig. 2b**). Similar results were obtained when the APC/C subunit CDC16 was depleted (data not shown).

When fixed cells were analyzed by microscopy, we observed an increase in the number of prometaphase and metaphase cells following APC15 depletion (**Fig. 2c** and **Supplementary Fig. 2**), consistent with a delay during these stages of mitosis. We could also detect an increase in the frequency of cells in anaphase and telophase, perhaps due to the larger number of cells analyzed ($n > 8{,}600$) compared to the number used in generating the live-cell imaging data ($n = 25$). The increase in mitotic index that was observed after APC15 depletion was partly restored by co-depletion of MAD2, consistent with the notion that APC15 depletion delays mitotic progression by compromising APC/C function (**Fig. 2d**).

APC15 is required for APC/C^{MCC} disassembly

Because APC/C is activated by CDC20 and inhibited by MAD2 and BUBR1, we asked whether APC15 depletion might alter APC/C function by affecting the steady-state levels of these proteins on the APC/C. Immunoblotting (**Fig. 3a**) or silver-staining (**Fig. 3b**) analyses revealed that the levels of all three proteins on the APC/C strongly increased following depletion of APC15, which indicated that APC15 depletion leads to accumulation of MCC on the APC/C. This effect was particularly evident when APC/C was isolated from cells that had been synchronized in prometaphase by nocodazole treatment (**Fig. 3a**, lane 8), but it could also be observed to a lesser extent in APC/C samples from asynchronous cell populations (**Fig. 3a**, lane 6). When MAD2 was co-depleted from cells at the same time as APC15, neither CDC20 nor BUBR1 accumulated on APC/C, which indicated that the increased binding of these proteins to the APC/C depends on the SAC (**Fig. 3b**, lane 7 compared to lane 8; **Fig. 3c**, lane 15 compared to lane 16).

To test whether the accumulation of CDC20, MAD2 and BUBR1 on the APC/C occurs specifically in mitosis, we released APC15-depleted cells from a thymidine-induced arrest in S phase, monitored cell cycle progression of cells stained with propidium iodide by fluorescence-activated cell sorting (FACS) (**Fig. 3d**) and analyzed the amounts of these proteins on the APC/C by immunoblotting (**Fig. 3e**). The strongest increase in CDC20, MAD2 and BUBR1 on the APC/C was observed when cells entered mitosis (**Fig. 3e**, lanes 13–16), which indicated that APC15 depletion leads to accumulation of MCC on the APC/C when the SAC becomes active.

Because a previous study[27] had found that MCC disassembly in cell extracts depends on APC/C activity, and APC15 could be required for APC/C activity, we next asked whether APC15 depletion might decrease MCC disassembly. We released APC15-depleted HeLa cells from nocodazole arrest and determined the levels of CDC20, MAD2 and BUBR1 on the APC/C over time. In control cells, the majority of MAD2 and BUBR1 was removed from the APC/C 90 min after the release (**Fig. 4a**, lane 10; **Fig. 4b**, lane 2). At that time, cells had begun to exit mitosis, as evidenced by a decrease in cyclin-B1 and an increase in the electrophoretic mobility of CDC27, indicative of its dephosphorylation (**Fig. 4a**, lane 2; **Fig. 4b**, lane 2). In contrast, in cells depleted of APC15, the levels of CDC20, MAD2 and BUBR1 remained high on the APC/C 90 min after the release (**Fig. 4a**, lane 13 compared to lane 14; **Fig. 4b**, lanes 5 and 6), and cyclin-B1 degradation and CDC27 dephosphorylation were reduced, though not abolished (**Fig. 4a**, lane 6; **Fig. 4b**, lane 6). Following APC15 depletion, all three MCC subunits could still be detected on the APC/C even 180 min after the release, although at greatly reduced levels (**Fig. 4a**, lane 15). These results indicate that APC15 is required for rapid MCC disassembly.

To confirm this notion, we analyzed MCC disassembly *in vitro* by incubating immunopurified APC/C^{MCC} with ubiquitin, the ubiquitin-activating enzyme E1 and the E2 enzyme UBCH10. Also in this assay, MCC disassembly was strongly decreased on APC/C^{MCC} isolated from APC15-depleted cells (**Fig. 4c**, lanes 6–8). These observations indicate that APC15 promotes progression through mitosis at least in part by facilitating MCC disassembly. We presently do not know whether the reduced rate of MCC disassembly observed in our assays is due to residual amounts of APC15 or whether MCC disassembly can also proceed slowly in the absence of APC15.

MCC disassembly depends on p31(comet)[29,32–34] and proteasome activity[32,48–50]. We compared the effects of APC15 depletion to the effects of p31(comet) depletion and proteasome inhibition. We released HeLa cells depleted of APC15 or p31(comet) or both from nocodazole arrest, in the presence or absence of proteasome inhibitor MG132 and analyzed CDC20, MAD2 and BUBR1 on the APC/C over time (**Supplementary Fig. 3**). APC15 depletion resulted in accumulation of

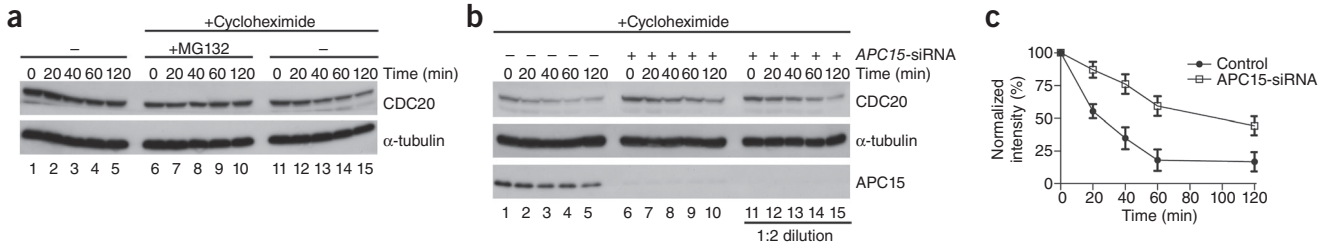

Figure 5 CDC20 turnover in prometaphase depends on APC15. (**a**) Western blot showing CDC20 degradation in control cells arrested in prometaphase by using nocodazole. Cells were treated with cycloheximide as indicated to block protein synthesis in the presence or the absence of the proteasome inhibitor MG132 for indicated times. (**b**) Western blot showing CDC20 degradation in prometaphase-arrested control- and *APC15*-siRNA–treated cells. Cells were incubated with cycloheximide to block protein synthesis for indicated times. (**c**) Mean CDC20 protein levels in cycloheximide-treated control and APC15-depleted HeLa cells ($n = 4$; error bars, s.e.m.). Signal intensity was normalized to α-tubulin levels.

much more MCC on APC/C than p31(comet) depletion did, although both treatments delayed MCC disassembly to a similar extent. It is possible that APC15 and p31(comet) were depleted to different degrees in our experiments or that p31(comet) acts catalytically in MCC disassembly and is therefore less sensitive to partial depletion than APC15, which is expected to function in a stoichiometric manner as an APC/C subunit. However, the different effects of APC15 and p31(comet) depletion are also consistent with the possibility that p31(comet) depletion affects MCC steady-state levels through two distinct mechanisms: (i) by 'capping' the MAD1–MAD2^C template at unattached kinetochores and thereby preventing MCC formation and (ii) by binding to MAD2^C as part of the MCC and thereby promoting MCC disassembly. In contrast, APC15 depletion might reduce MCC disassembly without slowing down MCC formation, thus leading to a more pronounced accumulation of MCC on the APC/C.

These experiments also confirmed that proteasome inhibition delays MCC disassembly. Like p31(comet) depletion, MG132 treatment led to only a small increase in MCC levels on the APC/C. However, in this case, the difference relative to depleting APC15 is presumably because the proteasome had only been inhibited during the last 3 h of the experiment, whereas cells had been gradually depleted of APC15 for a much longer period of time (48 h), during which MCC was able to accumulate. These observations indicate that MCC disassembly depends on at least three components: APC15, p31(comet) and proteasome activity.

APC15 is required for CDC20 degradation in prometaphase

APC15 depletion not only increased the amounts of CDC20 that were associated with the APC/C but also increased CDC20 steady-state levels in total cell lysates (**Fig. 3a**, lanes 2 and 4). This was not, or was only to a much lesser degree, the case for MAD2 and BUBR1, which implies that APC15 depletion might have two different effects: (i) a change in the equilibrium between APC/C-associated and non-associated MCC subunits and (ii) an increase in the cellular concentration of CDC20. Because CDC20 is continuously synthesized and degraded during prometaphase[30], we analyzed whether APC15 depletion might stabilize CDC20. As reported[30], CDC20 levels decreased in prometaphase-arrested cells when protein synthesis was inhibited by cycloheximide (**Fig. 5a**, lanes 11–15). This effect was reversed by MG132, which indicated that in cycloheximide-treated cells, CDC20 levels decrease due to proteolysis (**Fig. 5a**, lanes 6–10). Notably, the rate of this proteolysis was reduced in cells depleted of APC15, which indicated that APC15 is required for rapid degradation of CDC20 in cells with an active SAC (**Fig. 5b**, lanes 6–10; quantified in **Fig. 5c**).

APC15 is dispensable for APC/C^{CDC20} and APC/C^{CDH1} activity

One possible interpretation of the above results is that APC15 depletion would compromise APC/C activity, reducing CDC20 ubiquitylation and consequently delaying MCC disassembly. To test this possibility, we generated baculoviruses expressing all 14 subunits of the human APC/C, co-infected insect cells with them and isolated recombinant APC/C. The recombinant complexes contained a subunit pattern, as seen by

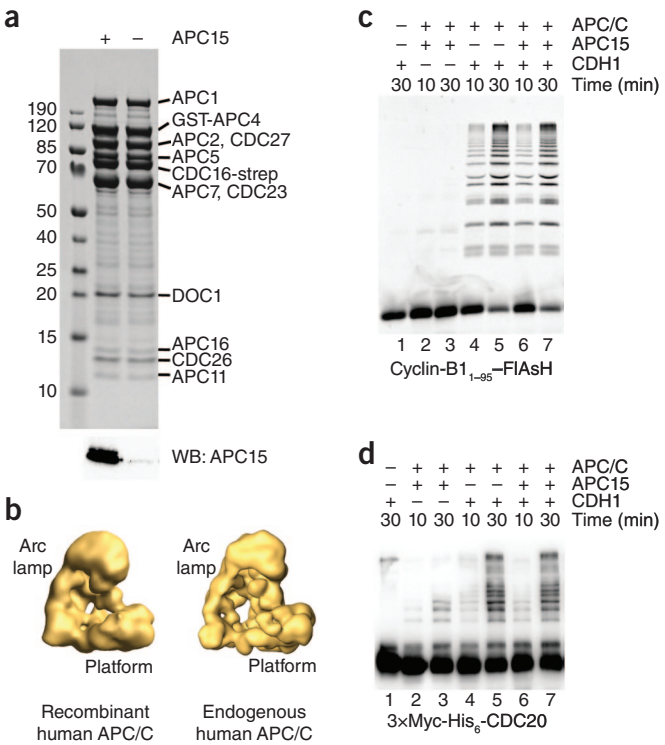

Figure 6 APC15 is not essential for cyclin-B1 and CDC20 ubiquitylation by APC/C^{CDH1}. (**a**) Coomassie stain (top) showing recombinant human APC/C as either wild-type complex or complex lacking the APC15 subunit (bottom, APC15 western blot). Identities of APC/C proteins and masses of molecular-weight markers (kDa) are indicated. GST, glutathione S-transferase tag; strep, streptavidin tag. (**b**) 3D models of recombinant and endogenous human apo-APC/C derived by negative-staining single-particle electron microscopy. (**c**) SDS-PAGE showing direct fluorescence of FlAsH-labeled N-terminal fragment of cyclin-B1 and cyclin-B1–ubiquitin conjugates. Ubiquitylation reactions were performed with recombinant human APC/C with or without APC15 and in the presence or absence of CDH1 as shown, with a ubiquitylation mixture containing UBCH10 and UBE2S. (**d**) Western blot showing recombinant CDC20 and CDC20–ubiquitin conjugates. Ubiquitylation reactions were as in **c**).

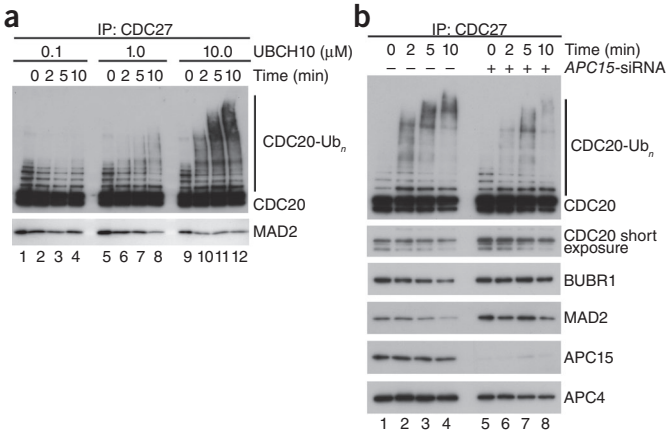

Figure 7 APC15 is required for CDC20 autoubiquitylation by APC/C^{MCC}. (**a**) Western blot showing CDC20 autoubiquitylation by APC/C^{MCC} immobilized on anti-CDC27–antibody beads incubated with increasing concentrations of UBCH10. After indicated time points, anti-CDC27–antibody beads were washed, and bound protein was eluted by using antigenic peptides. (**b**) Western blot showing CDC20 autoubiquitylation by wild-type or APC15-depleted APC/C^{MCC} immobilized on anti-CDC27–antibody beads incubated with 10 μM UBCH10. After indicated time points, anti-CDC27–antibody beads were washed, and bound protein was eluted by using antigenic peptides.

SDS-PAGE (**Fig. 6a**), that is reminiscent of APC/C purified from HeLa cells. Single-particle electron microscopy and angular reconstitution revealed that, at the resolution obtained, the overall shape of the recombinant complexes is indistinguishable from those of the three-dimensional (3D) models we have previously obtained for endogenous human APC/C (**Fig. 6b**; refs. 11,12). Furthermore, the recombinant complexes were able to ubiquitylate an N-terminal fragment of cyclin-B1 in a CDH1-dependent manner (**Fig. 6c**, lanes 6 and 7). Recombinant APC/C lacking APC11 was unable to mediate ubiquitylation reactions, which confirmed that this activity was attributable to human APC/C (**Supplementary Fig. 4**). These results indicate that the recombinant human APC/C which we have generated here is functional and similar in its properties to endogenous APC/C.

Next we generated recombinant APC/C lacking APC15 (**Fig. 6a**). To exclude that an APC15-related protein from insect host cells (from the moth *Spodoptera frugiperda*) could substitute for human APC15, we analyzed our sample by mass spectrometry and searched for peptides derived from the sequence of *S. frugiperda* APC15, which we had identified by BLAST searches (**Supplementary Fig. 1a**). No peptides from *S. frugiperda* APC15 could be detected (data not shown). Human APC/C can therefore be assembled in the complete absence of APC15. Nevertheless, recombinant APC/C lacking APC15, after incubation with CDH1, was similarly active in supporting the formation of cyclin-B1 and CDC20 ubiquitin conjugates as wild-type APC/C (**Fig. 6c**,**d**). Similar observations were made in ubiquitylation assays using a ubiquitin fusion to the cyclin-B1 fragment as a substrate to specifically assay E2 enzyme UBE2S instead of UBCH10 and in assays using CDC20 instead of CDH1 (**Supplementary Fig. 4c**).

APC15 mediates CDC20 autoubiquitylation by APC/C^{MCC}

Although our data cannot exclude the possibility that APC15 has an effect on kinetic properties of ubiquitylation reactions that cannot be detected by our assays, our results also show unequivocally that APC15 is not essential for the ubiquitylation activity of APC/C^{CDH1} and APC/C^{CDC20}. We thus tested whether APC15 is required for the ubiquitylation of CDC20 when this protein is part of APC/C^{MCC}. This reaction may depend on different mechanisms than substrate ubiquitylation mediated by APC/C^{CDH1} and APC/C^{CDC20}, similarly to how Cdc20 ubiquitylation by APC/C^{Cdh1} and Cdc20 autoubiquitylation have been shown to differ in yeast[51]. Because we were so far not able to reconstitute APC/C^{MCC} by using a fully recombinant system, we used APC/C^{MCC} isolated from APC15-depleted cells. We confirmed the finding by a previous study[27] that incubation of isolated APC/C^{MCC} with ubiquitin, E1 and UBCH10 resulted in ubiquitylation of CDC20 and in dissociation of MAD2 from APC/C^{MCC} (**Fig. 7a**). In contrast, CDC20 ubiquitylation was reduced when we used APC/C^{MCC} from which APC15 had been depleted (**Fig. 7b**, lanes 5–8). This reduction was consistently observed in all seven independent experiments performed (**Supplementary Fig. 5**), even though more CDC20 was present in the APC/C^{MCC} samples isolated from APC15-depleted cells than in samples containing wild-type APC/C^{MCC} (**Fig. 7b**, APC4 immunoblot signals compared to CDC20 signals in the shorter immunoblot exposure), and depletion of APC15 by RNAi may have been incomplete. These results indicate that APC15 is required for the efficient ubiquitylation of CDC20 when this protein is part of MCC but not when CDC20 is a substrate of APC/C^{CDH1}.

DISCUSSION

Because APC/C activity is essential for sister-chromatid separation and mitotic exit, APC/C has to be relieved from its inhibition by MCC once spindle assembly is completed. Here we confirm and extend the finding that C11ORF51 (APC15) is an APC/C subunit required for this event[38–40]. Notably, we show for the first time, to our knowledge, that APC15 is essential not only for rapid MCC disassembly but also for efficient CDC20 autoubiquitylation by APC/C^{MCC} and for subsequent proteasomal degradation in cells with an active SAC. This correlation supports the view that CDC20 ubiquitylation and degradation facilitate rapid MCC disassembly and APC/C activation[27,29]. Our results are not consistent with the proposal that CDC20 degradation maintains the checkpoint[30,40]. We therefore favor the model that CDC20 is constantly autoubiquitylated by APC/C^{MCC} and degraded in cells with an active checkpoint, which leads to continuous MCC disassembly.

According to this hypothesis, APC/C inhibition can only be maintained as long as newly synthesized CDC20 is assembled into MCCs. Once MCC production has ceased, newly synthesized CDC20 would rapidly replace MCC on APC/C, leading to APC/C activation. As first proposed by a previous study[29], checkpoint inhibition of the APC/C may therefore be achieved not by stable association of MCC with APC/C but by a dynamic equilibrium of MCC assembly and disassembly, which would lead to continuous turnover of MCC on APC/C.

This hypothesis has the potential to explain why CDC20 is continuously synthesized and degraded during prometaphase[30] and how APC/C is activated rapidly and by default in metaphase, although MAD2 binds to CDC20 tightly during prometaphase. The hypothesis also provides a rationale for a number of previous observations, such as the fact that inhibition of the proteasome leads to accumulation of MCC on APC/C[11,32,48–50]. Notably, the MCC-turnover hypothesis also implies that MCC's association with the APC/C is not only required for APC/C inhibition, as was previously assumed, but also may have the opposite function, namely to overcome APC/C's inhibition by MCC.

What may be the role of APC15 in this process? As a subunit of the APC/C, APC15 could simply be required for the ubiquitylation activity of the APC/C. However, we found that recombinant forms of human APC/C^{CDH1}, whose generation we report here, can ubiquitylate both cyclin-B1 and CDC20 similarly well in the presence or absence of APC15, which implies that APC/C's ubiquitylation activity *per se* does not strictly depend on APC15. On the contrary, the ability of APC/C^{MCC}

to autoubiquitylate CDC20 is reduced after depletion of APC15, which indicates that APC15 has a specific role in this process that is dispensable for substrate ubiquitylation by APC/C^{CDH1} and APC/C^{CDC20}. The location of APC15 in the platform domain may provide a rationale for this phenomenon, as our results indicate that APC15 is located in the vicinity of MCC's binding site. APC15 could therefore be required for proper positioning of MCC on the APC/C, an effect that could be required for CDC20 autoubiquitylation. Alternatively, APC15 could have effects on the catalytic core of the APC/C, and these effects could be required for CDC20 autoubiquitylation but dispensable for conventional substrate ubiquitylation.

Notably, APC15 is distantly related to Mnd2, an APC/C subunit that had previously been identified only in budding yeast and other fungi. This finding confirms the notion that APC/C is highly conserved among eukaryotes, a phenomenon that presumably reflects the early appearance of APC/C during evolution and the importance of APC/C's function and its tight regulation. Unlike APC15, Mnd2 was so far only known to have a role in meiosis I, in which Mnd2 functions as an inhibitor of the meiosis-specific APC/C coactivator Ama1 (refs. 52,53). However, because Ama1 is related in structure and function to CDC20, it is conceivable that Mnd2 and APC15 share the ability to control some property of APC/C coactivator proteins, a phenomenon that in the case of Mnd2 may lead to inactivation of Ama1 and in the case of APC15 to disassembly of MCC. It will, therefore, be interesting to test whether Mnd2 inhibits Ama1 by a mechanism that depends on Ama1 autoubiquitylation by APC/C^{Ama1}, similarly to how the presence of APC15 enables CDC20 autoubiquitylation by APC/C^{MCC}. Consistent with this possibility, and supporting the notion that APC15 and Mnd2 perform related functions, another study reported, after submission of this manuscript, that Mnd2 is also required for MCC-dependent Cdc20 autoubiquitylation and SAC inactivation in mitotic yeast cells[54].

METHODS

Methods and any associated references are available in the online version of the paper.

Accession codes. Data for recombinant human APC/C have been deposited in the Electron Microscopy Data Bank, with accession code EMD-2204.

Note: Supplementary information is available in the online version of the paper.

ACKNOWLEDGMENTS

Research in the laboratory of J.-M.P is supported by Boehringer Ingelheim, the Vienna Science and Technology Fund (WWTF LS09-13), the Laura Bassi Center for Optimized Structural Studies (FFG 822736) and the Austrian Science Fund (FWF special research program SFB F34 'Chromosome Dynamics', grant W1221 'DK: Structure and Interaction of Biological Macromolecules' and Wittgenstein award Z196-B20). Research in the laboratories of J.-M.P. and A.A.H. is supported by the European Community's Seventh Framework Programme (FP7/2007-2013) under grant agreement no. 241548 (MitoSys). Research in the laboratory of B.A.S. is supported by the American Lebanese Syrian Associated Charities/St. Jude and the Howard Hughes Medical Institute. Research in the laboratory of H. Stark is supported by the German Research Foundation (DFG) under grant agreement SFB860. Research in the laboratory of K.M. is supported by European Community's Seventh Framework Programme under grant agreement no. 262067 (PRIME-XS). Y.T. was supported by the Japan Society for the Promotion of Science (Postdoctoral Fellowship for Research Abroad). N.G.B. is supported as a Fellow of the Jane Coffin Childs Memorial Fund for Medical Research.

AUTHOR CONTRIBUTIONS

B.A.S. and J.-M.P. planned and supervised the project. K.U., B.T.D., H. Schutz, R.L., G.P., Y.T., M.A.J., N.G.B. and I.P. designed the experiments. K.U. performed experiments on APC15 function. B.T.D. and N.G.B. performed experiments on recombinant human APC/C. M.A.J. and G.P. established protocols for coactivator protein purification. H. Schutz performed experiments on APC15 being an APC/C core subunit. R.L. performed IFM experiments. G.P. performed antibody labeling and contributed to EM experiments. Y.T. performed time-lapse microscopy. I.P. and A.A.H. created LAP-tagged APC15. M.N. performed APC15 homology searches. K.M. performed mass spectrometry. H. Stark performed EM experiments, calculated 3D EM structures and analyzed APC15 antibody labeling. K.U., R.L., G.P., B.T.D., N.G.B., B.A.S. and J.-M.P. wrote the paper.

COMPETING FINANCIAL INTERESTS

The authors declare no competing financial interests.

Published online at http://www.nature.com/doifinder/10.1038/nsmb.2412.
Reprints and permissions information is available online at http://www.nature.com/reprints/index.html.

1. Musacchio, A. Spindle assembly checkpoint: the third decade. *Phil. Trans. R. Soc. Lond. B* **366**, 3595–3604 (2011).
2. Rieder, C.L., Cole, R.W., Khodjakov, A. & Sluder, G. The checkpoint delaying anaphase in response to chromosome monoorientation is mediated by an inhibitory signal produced by unattached kinetochores. *J. Cell Biol.* **130**, 941–948 (1995).
3. Stern, B.M. & Murray, A.W. Lack of tension at kinetochores activates the spindle checkpoint in budding yeast. *Curr. Biol.* **11**, 1462–1467 (2001).
4. Fang, G., Yu, H. & Kirschner, M.W. The checkpoint protein MAD2 and the mitotic regulator CDC20 form a ternary complex with the anaphase-promoting complex to control anaphase initiation. *Genes Dev.* **12**, 1871–1883 (1998).
5. Hwang, L.H. *et al.* Budding yeast Cdc20: a target of the spindle checkpoint. *Science* **279**, 1041–1044 (1998).
6. Kim, S.H., Lin, D.P., Matsumoto, S., Kitazono, A. & Matsumoto, T. Fission yeast Slp1: an effector of the Mad2-dependent spindle checkpoint. *Science* **279**, 1045–1047 (1998).
7. Kramer, E.R., Gieffers, C., Holzl, G., Hengstschlager, M. & Peters, J.M. Activation of the human anaphase-promoting complex by proteins of the CDC20/Fizzy family. *Curr. Biol.* **8**, 1207–1210 (1998).
8. Kramer, E.R., Scheuringer, N., Podtelejnikov, A.V., Mann, M. & Peters, J.M. Mitotic regulation of the APC activator proteins CDC20 and CDH1. *Mol. Biol. Cell* **11**, 1555–1569 (2000).
9. Peters, J.M. The anaphase-promoting complex: proteolysis in mitosis and beyond. *Mol. Cell* **9**, 931–943 (2002).
10. Dube, P. *et al.* Localization of the coactivator Cdh1 and the cullin subunit Apc2 in a cryo-electron microscopy model of vertebrate APC/C. *Mol. Cell* **20**, 867–879 (2005).
11. Herzog, F. *et al.* Structure of the anaphase-promoting complex/cyclosome interacting with a mitotic checkpoint complex. *Science* **323**, 1477–1481 (2009).
12. Buschhorn, B.A. *et al.* Substrate binding on the APC/C occurs between the coactivator Cdh1 and the processivity factor Doc1. *Nat. Struct. Mol. Biol.* **18**, 6–13 (2011).
13. Gmachl, M., Gieffers, C., Podtelejnikov, A.V., Mann, M. & Peters, J.M. The RING-H2 finger protein APC11 and the E2 enzyme UBC4 are sufficient to ubiquitinate substrates of the anaphase-promoting complex. *Proc. Natl. Acad. Sci. USA* **97**, 8973–8978 (2000).
14. Leverson, J.D. *et al.* The APC11 RING-H2 finger mediates E2-dependent ubiquitination. *Mol. Biol. Cell* **11**, 2315–2325 (2000).
15. Tang, Z. *et al.* APC2 Cullin protein and APC11 RING protein comprise the minimal ubiquitin ligase module of the anaphase-promoting complex. *Mol. Biol. Cell* **12**, 3839–3851 (2001).
16. Glotzer, M., Murray, A.W. & Kirschner, M.W. Cyclin is degraded by the ubiquitin pathway. *Nature* **349**, 132–138 (1991).
17. Pfleger, C.M. & Kirschner, M.W. The KEN box: an APC recognition signal distinct from the D box targeted by Cdh1. *Genes Dev.* **14**, 655–665 (2000).
18. Kraft, C., Vodermaier, H.C., Maurer-Stroh, S., Eisenhaber, F. & Peters, J.M. The WD40 propeller domain of Cdh1 functions as a destruction box receptor for APC/C substrates. *Mol. Cell* **18**, 543–553 (2005).
19. da Fonseca, P.C. *et al.* Structures of APC/C(Cdh1) with substrates identify Cdh1 and Apc10 as the D-box co-receptor. *Nature* **470**, 274–278 (2011).
20. Chao, W.C., Kulkarni, K., Zhang, Z., Kong, E.H. & Barford, D. Structure of the mitotic checkpoint complex. *Nature* **484**, 208–213 (2012).
21. Sudakin, V., Chan, G.K. & Yen, T.J. Checkpoint inhibition of the APC/C in HeLa cells is mediated by a complex of BUBR1, BUB3, CDC20, and MAD2. *J. Cell Biol.* **154**, 925–936 (2001).
22. Luo, X., Tang, Z., Rizo, J. & Yu, H. The Mad2 spindle checkpoint protein undergoes similar major conformational changes upon binding to either Mad1 or Cdc20. *Mol. Cell* **9**, 59–71 (2002).
23. Sironi, L. *et al.* Crystal structure of the tetrameric Mad1-Mad2 core complex: implications of a 'safety belt' binding mechanism for the spindle checkpoint. *EMBO J.* **21**, 2496–2506 (2002).
24. De Antoni, A. *et al.* The Mad1/Mad2 complex as a template for Mad2 activation in the spindle assembly checkpoint. *Curr. Biol.* **15**, 214–225 (2005).
25. Mapelli, M., Massimiliano, L., Santaguida, S. & Musacchio, A. The Mad2 conformational dimer: structure and implications for the spindle assembly checkpoint. *Cell* **131**, 730–743 (2007).
26. Burton, J.L. & Solomon, M.J. Mad3p, a pseudosubstrate inhibitor of APCCdc20 in the spindle assembly checkpoint. *Genes Dev.* **21**, 655–667 (2007).
27. Reddy, S.K., Rape, M., Margansky, W.A. & Kirschner, M.W. Ubiquitination by the anaphase-promoting complex drives spindle checkpoint inactivation. *Nature* **446**, 921–925 (2007).

28. Miniowitz-Shemtov, S., Teichner, A., Sitry-Shevah, D. & Hershko, A. ATP is required for the release of the anaphase-promoting complex/cyclosome from inhibition by the mitotic checkpoint. *Proc. Natl. Acad. Sci. USA* **107**, 5351–5356 (2010).
29. Varetti, G., Guida, C., Santaguida, S., Chiroli, E. & Musacchio, A. Homeostatic control of mitotic arrest. *Mol. Cell* **44**, 710–720 (2011).
30. Nilsson, J., Yekezare, M., Minshull, J. & Pines, J. The APC/C maintains the spindle assembly checkpoint by targeting Cdc20 for destruction. *Nat. Cell Biol.* **10**, 1411–1420 (2008).
31. Gao, Y.F. *et al.* Cdk1-phosphorylated CUEDC2 promotes spindle checkpoint inactivation and chromosomal instability. *Nat. Cell Biol.* **13**, 924–933 (2011).
32. Jia, L. *et al.* Defining pathways of spindle checkpoint silencing: functional redundancy between Cdc20 ubiquitination and p31(comet). *Mol. Biol. Cell* **22**, 4227–4235 (2011).
33. Teichner, A. *et al.* p31comet promotes disassembly of the mitotic checkpoint complex in an ATP-dependent process. *Proc. Natl. Acad. Sci. USA* **108**, 3187–3192 (2011).
34. Westhorpe, F.G., Tighe, A., Lara-Gonzalez, P. & Taylor, S.S. p31comet-mediated extraction of Mad2 from the MCC promotes efficient mitotic exit. *J. Cell Sci.* **124**, 3905–3916 (2011).
35. Miniowitz-Shemtov, S. *et al.* Role of phosphorylation of Cdc20 in p31(comet)-stimulated disassembly of the mitotic checkpoint complex. *Proc. Natl. Acad. Sci. USA* **109**, 8056–8060 (2012).
36. Xia, G. *et al.* Conformation-specific binding of p31(comet) antagonizes the function of Mad2 in the spindle checkpoint. *EMBO J.* **23**, 3133–3143 (2004).
37. Yang, M. *et al.* p31comet blocks Mad2 activation through structural mimicry. *Cell* **131**, 744–755 (2007).
38. Kittler, R. *et al.* Genome-scale RNAi profiling of cell division in human tissue culture cells. *Nat. Cell Biol.* **9**, 1401–1412 (2007).
39. Hubner, N.C. *et al.* Quantitative proteomics combined with BAC TransgeneOmics reveals in vivo protein interactions. *J. Cell Biol.* **189**, 739–754 (2010).
40. Mansfeld, J., Collin, P., Collins, M.O., Choudhary, J.S. & Pines, J. APC15 drives the turnover of MCC-CDC20 to make the spindle assembly checkpoint responsive to kinetochore attachment. *Nat. Cell Biol.* **13**, 1234–1243 (2011).
41. Hutchins, J.R. *et al.* Systematic analysis of human protein complexes identifies chromosome segregation proteins. *Science* **328**, 593–599 (2010).
42. Kops, G.J. *et al.* APC16 is a conserved subunit of the anaphase-promoting complex/cyclosome. *J. Cell Sci.* **123**, 1623–1633 (2010).
43. Cheeseman, I.M. & Desai, A. A combined approach for the localization and tandem affinity purification of protein complexes from metazoans. *Sci. STKE* **2005**, pl1 (2005).
44. Poser, I. *et al.* BAC TransgeneOmics: a high-throughput method for exploration of protein function in mammals. *Nat. Methods* **5**, 409–415 (2008).
45. Zachariae, W. *et al.* Mass spectrometric analysis of the anaphase-promoting complex from yeast: identification of a subunit related to cullins. *Science* **279**, 1216–1219 (1998).
46. Hall, M.C., Torres, M.P., Schroeder, G.K. & Borchers, C.H. Mnd2 and Swm1 are core subunits of the *Saccharomyces cerevisiae* anaphase-promoting complex. *J. Biol. Chem.* **278**, 16698–16705 (2003).
47. Schreiber, A. *et al.* Structural basis for the subunit assembly of the anaphase-promoting complex. *Nature* **470**, 227–232 (2011).
48. Visconti, R., Palazzo, L. & Grieco, D. Requirement for proteolysis in spindle assembly checkpoint silencing. *Cell Cycle* **9**, 564–569 (2010).
49. Zeng, X. *et al.* Pharmacologic inhibition of the anaphase-promoting complex induces a spindle checkpoint-dependent mitotic arrest in the absence of spindle damage. *Cancer Cell* **18**, 382–395 (2010).
50. Ma, H.T. & Poon, R.Y. Orderly inactivation of the key checkpoint protein mitotic arrest deficient 2 (MAD2) during mitotic progression. *J. Biol. Chem.* **286**, 13052–13059 (2011).
51. Foe, I.T. *et al.* Ubiquitination of Cdc20 by the APC occurs through an intramolecular mechanism. *Curr. Biol.* **21**, 1870–1877 (2011).
52. Oelschlaegel, T. *et al.* The yeast APC/C subunit Mnd2 prevents premature sister chromatid separation triggered by the meiosis-specific APC/C-Ama1. *Cell* **120**, 773–788 (2005).
53. Penkner, A.M., Prinz, S., Ferscha, S. & Klein, F. Mnd2, an essential antagonist of the anaphase-promoting complex during meiotic prophase. *Cell* **120**, 789–801 (2005).
54. Foster, S.A. & Morgan, D.O. The APC/C subunit Mnd2/Apc15 promotes Cdc20 autoubiquitination and spindle assembly checkpoint inactivation. *Mol. Cell* published online, doi:10.1016/j.molcel.2012.07.031 (30 August 2012).

ONLINE METHODS

Cell culture. HeLa cells were grown in DMEM including 10% FBS (Invitrogen), 2 mM L-glutamine and 100 μg ml^{-1} penicillin/streptomycin (both from Sigma) and plated on 6-well plates, containing 22-mm-diameter coverslips for immunofluorescence microscopy (IFM), or on 15-cm tissue-culture dishes. Cells were arrested in S phase by addition of 2.5 mM thymidine for 24 h. To obtain mitotic cells with an active checkpoint, cells were incubated with 100 nM nocodazole (Sigma) for 14 h and collected by mitotic shake-off. For proteasome inhibition, 10 μM MG132 (Sigma) was used. Protein synthesis was inhibited by adding 20 μg ml^{-1} cycloheximide (Sigma) as described[30].

RNA interference. HeLa cells were transfected with Lipofectamine RNAiMAX (Invitrogen) and 40 nM siRNA oligonucleotides for 48 h before analysis by immunoblotting or IFM (C11_2, 5′-UCGCGGAGAAAGACAACAA-3′; C11_3, 5′-GGACAUGGAAGGCAACGAA-3′; C11_4, 5′-GGAUCGACCCUGUGUGGAA-3′ (Ambion). MAD2, 5′-UUACUCGAGUGCAGAAAUA-3′; p31(comet), 5′-GGACACUAGUACCGCGAGU-3′ (Dharmacon). C11_4 siRNA was used unless otherwise indicated. GL2 luciferase was used as control siRNA[55]. APC15 and firefly luciferase esiRNAs (obtained as a kind gift from F. Buchholz, Max Planck Institute for Molecular Cell Biology and Genetics, Dresden, Germany) were used in **Figure 2a**,**b**.

Antibodies and immunoprecipitation. Polyclonal APC15 antibodies were generated by Gramsch Laboratories against a synthetic peptide (DEMNDYNESPDDGEV). APC2, CDC27, APC4, APC16, MAD2, BUBR1, CDC20 and GFP antibodies were described before[7,11,41]. In addition, the following commercial antibodies were used: CDC20 (1:200, sc-13162, Santa Cruz Biotechnology); cyclin-B1 (1:1,000, sc-245, monoclonal GNS1, Santa Cruz Biotechnology); α-tubulin (1:10,000, B-512, Sigma; 1:100, F2168, Sigma); BUB1 (1:500, MBL International); pH3Ser10 (1:1,000, 06-570, Millipore); anti–mouse IgG–HRP and anti–rabbit IgG–HRP (1:5,000, GE Healthcare); and anti-mouse and anti-rabbit–Alexa Fluor 568 and 647 (1:1,000, Invitrogen). APC/C was affinity purified from HeLa cells by using beads cross-linked to anti-CDC27 antibody (Affi-prep protein A beads, Bio-Rad). Cells were lysed for 30 min at 4 °C in lysis buffer (CytoBuster supplemented with 20 mM β-glycerophosphate, 10 mM Na-pyrophosphate, 10 mM NaF, 1 mM Na_3VO_4, 1 μM okadaic acid, 1× complete protease inhibitor cocktail (Roche)). Beads were washed three times in washing buffer (20 mM Tris, pH 7.5, 150 mM NaCl, 10% (v/v) glycerol, 0.1% (v/v) Tween-20). APC/C was recovered by elution with two bead volumes of 1 mg ml^{-1} antigenic peptide dissolved in elution buffer (20 mM Tris, pH 7.5, 150 mM NaCl, 10% (v/v) glycerol, 0.1% (w/v) octyl-β-D-glucopyranoside) or 100 mM glycine-HCl at pH 2.2.

CDC20 autoubiquitylation by APC/C^{MCC} and *in vitro* MCC disassembly. *In vitro* MCC dissociation and CDC20 autoubiquitylation was adopted from another study[27], with the following changes. APC/C purified from prometaphase-arrested HeLa cells was immobilized on anti-CDC27–antibody beads and incubated with 10 μM UbcH10, 0.5 μM E1, 1.5 mg ml^{-1} ubiquitin (Sigma), 30 mM Tris, pH 7.5, 100 mM KCl, 2 mM $MgCl_2$, 0.1 mM $CaCl_2$, ATP-regenerating system (7.5 mM creatine phosphate, 1 mM ATP, 1 mM $MgCl_2$), 10 mM dithiothreitol and 1 mg ml^{-1} BSA. The reactions were incubated at 23 °C with 1,000 r.p.m. shaking for indicated time points. After incubation with the ubiquitylation mixture, the anti-CDC27–antibody beads were washed, and bound protein was recovered by elution with antigenic peptide.

Time-lapse microscopy. HeLa cells stably expressing histone H2B-mCherry and mouse TUBB-LAP were used for live-cell imaging analysis (histone H2B-mCherry plasmid was a gift from J. Ellenberg, EMBL, Heidelberg, Germany). Cells were reverse transfected with 100 nM esiRNA by using Oligofectamine reagent (Invitrogen). The cells were cultured in an 8-well chamber (μ-Slide 8 well, ibidi GmbH) and filmed 48 h after transfection, on a DeltaVision sectioning microscope system equipped with an IX71 microscope (Olympus) and a CoolSnap HQ CCD camera (Photometrics). Time-lapse images were taken at 5-min intervals as 13 sections with 1-μm *z* steps, deconvolved and maximally projected. Cell-cycle stages were manually annotated to measure the duration of mitosis (from NEBD until anaphase onset) and mitotic exit (from anaphase until loss of microtubule bridges).

Immunofluorescence microscopy. Cells were fixed in 4% (w/v) paraformaldehyde in PBS, permeabilized in 0.1% (v/v) Triton X-100 in PBS, blocked with 3% (w/v) BSA in 0.01%TX-100/PBS and incubated with antibodies in blocking solution as described in figure legends. Images were taken on a Zeiss Axioplan 2 microscope with a 20× Plan-Neofluar objective lens, to determine mitotic indices, or on a Zeiss LSM700 confocal microscope with a 63× Plan-Apochromat objective lens at 0.38 μm *z* distance, to determine submitotic stages.

Data quantification and analysis. Western blot signals were quantified by using ImageJ (rsb.info.nih.gov/ij). Quantification data of western blots, live-cell imaging and IFM were processed with Microsoft Excel 2007 and GraphPad Prism 5.

Electron microscopy and antibody labeling. Purified apo-APC/C was incubated with submolar concentrations of anti-APC15 antibody and subjected to GraFix[56]. APC/C–antibody complexes were adsorbed to a thin film of carbon, transferred to an electron-microscopic grid covered with a perforated carbon film, stained with 2% (w/v) uranyl formate and air dried at room temperature. Images were recorded at a magnification of 88,000× on a 4,000 × 4,000 CCD camera (TVIPS GmbH) using two-fold pixel binning (1.8 Å per pixel) in a Philips CM200 FEG electron microscope (Philips/FEI) operated at 160-kV acceleration voltage. Antibody-labeled APC/C complexes were analyzed as described[11].

Expression and purification of recombinant human APC/C. Recombinant APC/C was expressed in insect cells (High Five SFM-adapted, Invitrogen) by using the Bac to Bac baculovirus system (Invitrogen). Full-length open reading frames of individual human APC/C subunits (APC1, APC2, APC3/CDC27, APC5, APC7, APC8/CDC23, APC10/DOC1, APC11, APC13, APC15, APC16 and CDC26) were PCR amplified from cDNAs obtained (Open Biosystems) and cloned into pFastBac-1. A construct encoding APC6/CDC16 bearing a C-terminal fusion to a TEV cleavage site (GSENLYFQ) followed by two copies of StrepTagII (GSWSHPQFEKGSWSHPQFEK) was produced by cloning a PCR product generated with primers including the fusion sequences. APC4 was cloned into a pFastBac-1 derivative encoding an N-terminal GST tag followed by a TEV protease cleavage site. All clones were verified by DNA sequencing. Bacmids encoding each subunit were generated by transposition of DH10Bac *Escherichia coli* (Invitrogen). Baculoviruses were produced by transfection of SF9 cells with FuGENE HD (Promega). P3 amplifications were used for all protein production. To express APC/C, High Five cells (Invitrogen) at a density of 1 × 10^6 ml^{-1} were co-infected with the 14 baculoviruses encoding the individual APC/C subunits, omitting the virus encoding APC15 as indicated. Cells were incubated post-infection for 24 h at 27 °C and two days at 20 °C. APC/C was prepared from infected cells by a two-step affinity purification procedure, first using the strep tag fused to APC6 and then the GST tag fused to APC4. All steps were conducted at 4 °C. Cells were collected by centrifugation at 1,000*g* for 10 min and lysed by sonication in APC/C buffer (20 mM Tris, pH 7.6, 150 mM NaCl, 1 mM DTT) containing complete EDTA-free protease inhibitors (Roche). Lysates were cleared by centrifugation at 15,000 r.p.m. in an SS-34 rotor for 30 min, and the supernatant was incubated with Strep-Tactin–agarose (IBA) for 1 h with agitation. Beads were transferred to a gravity-flow column and washed with 10 column volumes of APC/C buffer. APC/C was eluted with 6 column volumes of buffer containing 2.5 mM desthiobiotin, passed over a glutathione-Sepharose column by gravity flow, washed with 5 column volumes of APC/C buffer and eluted in APC/C buffer containing 10 mM reduced glutathione. The presence of all APC/C subunits was verified by mass spectrometry.

Recombinant APC/C ubiquitylation assays. Recombinant APC/C was assayed for ubiquitylation activity by using a modification of a previously described method[57]. Immediately after preparation on ice, 6.5 μl of a 'ubiquitylation mix' (190 nM E1, 190 nM UbcH10, 190 nM Ube2s, 1.5 mg ml^{-1} ubiquitin, 0.8 mg ml^{-1} BSA, 85 mM creatine phosphate, 12 mM ATP, 13 mM $MgCl_2$, 5 mM Tris, pH 7.5, 9 mM NaCl) was added to a 7-μl mixture of 80 nM recombinant APC/C and 2 μM substrate with or without 2 μM 3×Myc-His_6-CDH1, as indicated in figures. Reactions were incubated at 25 °C with 800 r.p.m. shaking in a Thermomixer R (Eppendorf) for the indicated times and stopped by adding an equal volume of 2× Laemmli buffer without DTT. To distinguish between ubiquitin chain initiation and elongation, reactions were carried out with a fluorescently labeled N-terminal fragment of cyclin-B1 or a fusion of ubiquitin to a fragment of cyclin-B1, UbcH10 or Ube2S and either CDH1 or CDC20 (**Supplementary Note**). These reactions were carried out at room temperature with 9 nM APC/C, 120 nM substrate, 1 μM coactivator in 15 mM Tris, 100mM NaCl, 5 mM MgATP, 0.25 mg ml^{-1} BSA,

doi:10.1038/nsmb.2412

190 nM E1, 190 nM of either E2 and initiated by addition of 125 μM ubiquitin. Reactions were separated by SDS-PAGE, and FlAsH fluorescence was detected with a Storm 860 imager (Molecular Dynamics). To monitor 3×Myc-His_6-CDC20 assays, samples were separated by SDS-PAGE on 12% polyacrylamide gels and western blotted with an anti-CDC20 antibody (1:200, ab64877 Abcam).

55. Elbashir, S.M. *et al*. Duplexes of 21-nucleotide RNAs mediate RNA interference in cultured mammalian cells. *Nature* **411**, 494–498 (2001).
56. Kastner, B. *et al*. GraFix: sample preparation for single-particle electron cryomicroscopy. *Nat. Methods* **5**, 53–55 (2008).
57. Williamson, A., Jin, L. & Rape, M. Preparation of synchronized human cell extracts to study ubiquitination and degradation. *Methods Mol. Biol.* **545**, 301–312 (2009).